

Vibrational Properties of Polyanionic Hydrides SrAl₂H₂ and SrAlSiH: New Insights into Al–H Bonding Interactions

Myeong H. Lee,[†] Otto F. Sankey,[†] Thomas Björling,[‡] David Moser,[‡] Dag Noréus,[‡]
Stewart F. Parker,[§] and Ulrich Häussermann^{*||}

Department of Physics, Arizona State University, P.O. Box 871504, Tempe, Arizona 85287-1504,
Structural Chemistry, Stockholm University, SE-10691 Stockholm, Sweden, ISIS Facility,
Rutherford Appleton Laboratory, Chilton, Didcot, Oxon OX11 0QX, U.K., and
Department of Chemistry and Biochemistry, Arizona State University,
P.O. Box 871604, Tempe, Arizona 85287-1604

Received April 16, 2007

The vibrational properties of the recently discovered aluminum hydrides SrAl₂H₂ and SrAlSiH have been investigated by means of inelastic neutron scattering (INS) and first-principles calculations. Both compounds contain Al–H units being part of a two-dimensional polyanionic layer, [(AlH)(AlH)]²⁻ and [Si(AlH)]²⁻, respectively. The INS spectrum of SrAlSiH is characterized by very weakly dispersed Al–H modes with well-resolved overtones, while SrAl₂H₂ yields a solid-state dispersed phonon spectrum. The frequency of the stretching mode of the Al–H unit in SrAlSiH is the hitherto lowest observed for a terminal Al–H bond. At the same time, SrAlSiH displays the highest decomposition temperature known for an aluminum hydride compound. It is proposed that the stability of solid-state aluminum hydrides correlates inversely with the strength of Al–H bonding.

1. Introduction

Aluminum hydrides play a central role in the quest for hydrogen storage materials. Much effort has been devoted to transform aluminates, which are aluminum hydrides of alkali and alkaline-earth metals, into technologically applicable materials.^{1–4} Characteristically, aluminates represent fully hydrogenated systems with tetrahedral [AlH₄] (as, e.g., in LiAlH₄) or octahedral [AlH₆] entities (as, e.g., in Na₃AlH₆). Recently, however, new main-group metal aluminum hydrides have emerged that are not fully hydrogenated.^{5,6} Instead, [Al–H] entities are part of a polyanion where Al is

bonded to either further Al atoms or other p-block metallic or semimetallic elements. Such polyanionic hydrides provide unforeseen coordination environments and bonding situations for H, which are intriguing from a fundamental point of view but also bear a high potential for interesting material properties. Bonding properties and lattice dynamics of polyanionic hydrides have not been explored yet. In this paper, we report on the vibrational properties of SrAl₂H₂ and SrAlSiH and their possible implication for a deeper understanding of Al–H bonding interactions in solid-state materials.

Trigonal SrAl₂H₂ (space group $P\bar{3}m1$) features a two-dimensional polyanion [Al₂H₂]²⁻ in which Al atoms are arranged as a puckered graphitic layer with three nearest neighbors (Figure 1a).⁵ A fourth coordination is taken by H, and the compound appears charge-balanced when assigning the oxidation state I⁻ for four-bonded Al. The structure of SrAlSiH is very similar to that of SrAl₂H₂: Half of the [Al–H] entities in the polyanionic layer of SrAl₂H₂ are replaced by isoelectronic Si (Figure 1b).⁶ This replacement occurs in a strictly ordered way; i.e., each Si atom is surrounded by three [Al–H] entities and vice versa. In SrAlSiH, the center of inversion present in SrAl₂H₂ is lost and the space group symmetry is reduced to $P3m1$.

* To whom correspondence should be addressed. E-mail: ulrich.hausermann@asu.edu.

[†] Department of Physics, Arizona State University.

[‡] Stockholm University.

[§] Rutherford Appleton Laboratory.

^{||} Department of Chemistry and Biochemistry, Arizona State University.

(1) Züttel, A. *Naturwissenschaften* **2004**, 91.

(2) Ritter, J. A.; Ebner, A. D.; Wang, J.; Zidan, R. *Mater. Today* **2003**, Sept, 18.

(3) Schüth, F.; Bogdanovic, B.; Felderhoff, M. *Chem. Commun.* **2004**, 2243.

(4) Bogdanovic, B.; Felderhoff, M.; Pommerin, A.; Schüth, F.; Spielkamp, N. *Adv. Mater.* **2006**, 18, 1198.

(5) Gingl, F.; Vogt, T.; Akiba, E. *J. Alloys Compd.* **2000**, 306, 127.

(6) Björling, T.; Noréus, D.; Jansson, K.; Andersson, M.; Leonova, E.; Edén, M.; Hälenius, U.; Häussermann, U. *Angew. Chem., Int. Ed.* **2005**, 44, 7269.

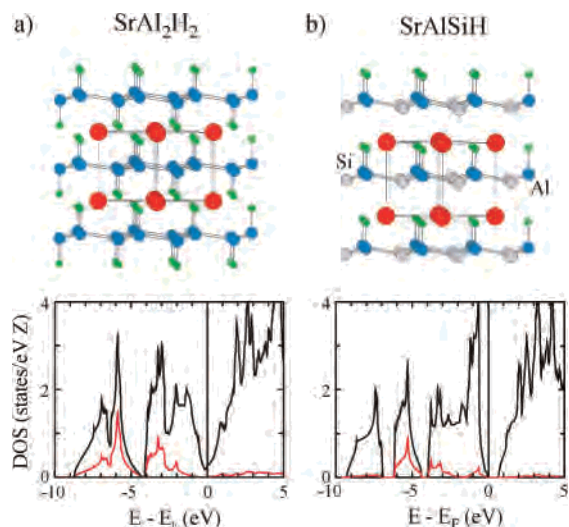


Figure 1. Crystal structures and electronic density of states of SrAl₂H₂ (a) and SrAlSiH (b). Red, blue, gray, and green circles denote Sr, Al, Si, and H atoms, respectively. The red curve in the density of states represents the contribution from H.

In both crystal structures, puckered hexagon nets formed by p-block elements are stacked in the same orientation on top of each other and sandwich Sr atoms in between. The local coordination of H is the same; however, the isoelectronic replacement of Al–H by Si has drastic consequences on the electronic structure and properties: SrAl₂H₂ is a metallic conductor, whereas for SrAlSiH a gap is opened in the density of states at the Fermi level ($E_g = 0.63$ eV), which makes the compound a unique example of a narrow-gap semiconductor hydride (Figure 1). Additionally, thermal stability is raised dramatically. The hydrogen desorption temperature of SrAlSiH exceeds 650 °C (1 atm) and is the highest known for aluminum hydride compounds.⁶ The most conspicuous difference between the two structures is that in SrAlSiH Sr is only coordinated by three H atoms. The Sr–H distance in SrAlSiH is considerably shorter than that in SrAl₂H₂ (2.48 vs 2.65 Å) and the Al–H distance significantly larger (1.77 vs 1.71 Å). Additionally, in SrAlSiH, [Al–H] entities are well-separated, while in SrAl₂H₂, H atoms approach each other at a distance of 2.77 Å.

To gain insight into the origin of the stunningly different properties of isoelectronic SrAl₂H₂ and SrAlSiH, we characterized the vibrational properties of the two hydrides by a combined inelastic neutron scattering (INS) and computational study. INS provides a unique form of vibrational spectroscopy. Unlike optical spectroscopy, there are no symmetry-based selection rules and all modes are allowed. Furthermore, the intensity of the modes is proportional to the amplitude of the motion (displacement) and the scattering cross section of the atoms involved. Compared to all other elements, the cross section of H is extremely large, which makes INS a superb probe for investigating H motion.^{7–9}

(7) Mitchell, P. C. H.; Parker, S. F.; Ramirez-Cuesta, A. J.; Tomkinson, J. *Vibration Spectroscopy with Neutrons—With Applications in Chemistry, Biology, Materials Science and Catalysis*; Series on Neutron Techniques and Applications; World Scientific: Hackensack, NJ, 2005; Vol. 3.

(8) Kearley, G. J. *Spectrochim. Acta* **1992**, *48A*, 349.

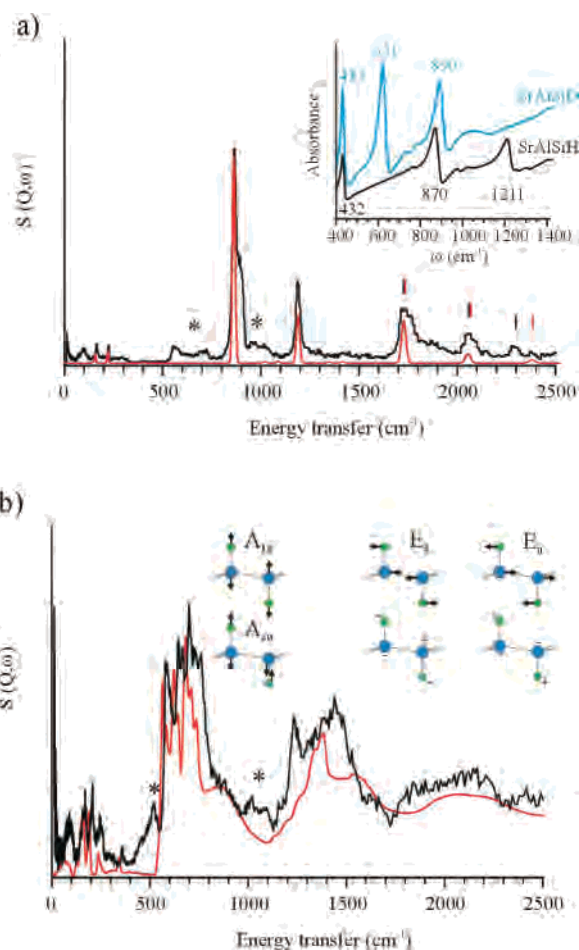


Figure 2. Measured (black line) and calculated (red line) INS spectra of SrAlSiH (a) and SrAl₂H₂ (b). The calculation for SrAlSiH corresponds to a Γ -point-only treatment. Intensities from impurities are marked with asterisks. Vertical markers in part a indicate the location of overtone maxima. The insets show the IR spectra of SrAlSiH and SrAlSiD (a) and the normal modes of external vibrations for SrAl₂H₂ (b). The calculated frequencies for SrAlSiH are slightly scaled (cf. Table 2 for the actual calculated values).

2. Experimental and Computational Details

SrAl₂H₂ was prepared by hydrogenating the orthorhombic Zintl phase SrAl₂ at mild conditions (around 200 °C and 50 bar of H₂) for 24 h. SrAl₂, in turn, was prepared by arc-melting stoichiometric amounts of Sr and Al. SrAlSiH was obtained from a mixture of SrH₂, Al, and Si, which was pressed to a pellet and hydrogenated (70 bar of H₂) at 700 °C for 24 h. This synthesis procedure is different compared to our previous one, where SrAlSiH was obtained by hydrogenating the alloy SrAlSi.⁶

The INS spectra of the two hydrides were measured at 20 K on the high-resolution time-of-flight spectrometer TOSCA at the pulsed neutron spallation source ISIS (U.K.), accessing an energy transfer from 0 to 4000 cm⁻¹. Both spectra (Figure 2) revealed an impurity, which in the case for SrAlSiH corresponds to SrH₂.¹⁰ The impurity in the SrAl₂H₂ sample could not be identified unambiguously but may be Sr₂AlH₇, which was reported to form when hydrogenating SrAl₂ at temperatures above 230 °C.⁵

Theoretical calculations were performed within the density functional theory with a plane-wave basis set in the VASP¹¹ code.

(9) Kearley, G. J. *Nucl. Instrum. Methods Phys. Res., Sect A* **1995**, *354*, 53.

(10) Colognesi, D.; Barrera, G.; Ramirez-Cuesta, A. J.; Zoppi, M. *J. Alloys Compd.* **2007**, *427*, 18.

Table 1. Computationally Relaxed Structural Parameters for SrAl₂H₂ (P3m1) and SrAlSiH (P3m1) Compared with Experimental Parameters

| SrAl ₂ H ₂ | PP-GGA | exptl ⁵ |
|--|--------|--------------------|
| <i>a</i> (Å) | 4.5267 | 4.5283 |
| <i>c</i> (Å) | 4.7195 | 4.7215 |
| Al(¹ / ₃ , ² / ₃ , <i>z</i>) | 0.4613 | 0.4589 |
| H(¹ / ₃ , ² / ₃ , <i>z</i>) | 0.0978 | 0.0976 |
| SrAlSiH | PP-GGA | exptl ⁶ |
| <i>a</i> (Å) | 4.2113 | 4.2139 |
| <i>c</i> (Å) | 4.9516 | 4.9550 |
| Al(² / ₃ , ¹ / ₃ , <i>z</i>) | 0.5396 | 0.547 |
| Si(¹ / ₃ , ² / ₃ , <i>z</i>) | 0.4452 | 0.431 |
| H(² / ₃ , ¹ / ₃ , <i>z</i>) | 0.8939 | 0.904 |

Ultrasoft pseudopotentials were used¹² to remove the core electrons, and only the s and p valence electrons are treated explicitly in the calculations. For Sr semicore p electrons were also included. For exchange and correlation, we used the generalized gradient approximation (GGA) of Perdew and Wang.¹³ We optimized both the lattice constants and internal coordinates for the unit cell to have zero pressure and zero force. The relaxed structural parameters agreed very well with the experimentally determined ones (Table 1). The *k*-point sampling of the Brillouin zone was an 8 × 8 × 8 Monkhorst–Pack grid.¹⁴

The phonon dispersion curves are obtained by a direct method^{15,16}—using supercells. A 3a × 3a × 3c supercell was generated. The internal coordinates of the supercell were reoptimized using the Γ point for SrAlSiH and a 2 × 2 × 2 sampling for metallic SrAl₂H₂. In the direct method, a force-constant matrix is obtained by displacing atoms, one at a time, by a small distance in each of the Cartesian directions. Each atom in the supercell was displaced by 0.01 Å along each *x*, *y*, and *z* direction, and the Hellmann–Feynman force acting on each atom of the supercell was determined. The force-constant matrix is determined by dividing the force by the displacement. Symmetry is used to reduce the number of needed displacements. The procedure is repeated for both positive and negative displacements, and the resulting spring constants are averaged (removing cubic anharmonicity). More computational details can be found in ref 16. The wavevector-dependent dynamical matrix was constructed assuming a finite range of interaction (less than half of the supercell dimensions) and diagonalized, which yields normal-mode frequency and eigenvectors. These results have been used to calculate the INS spectra by the aCLIMAX program.¹⁷

3. Results and Discussion

The INS spectra of SrAlSiH and SrAl₂H₂ are shown in Figure 2 for the range between 0 and 2500 cm⁻¹. Intensities arising from impurities are marked with asterisks. The spectrum of SrAlSiH is characterized by two narrow high-intensity bands at around 850 and 1200 cm⁻¹ and well-resolved overtones above 1500 cm⁻¹, while SrAl₂H₂ yields a solid-state dispersed vibrational spectrum. The high-intensity INS bands of SrAlSiH can unambiguously be assigned to [Al–H] bending and stretching modes, respectively. This follows from a comparison of the IR spectra of SrAlSiH and SrAlSiD (inset in Figure 2a), which display three bands at 432 (432), 870 (621), and 1211 (890) cm⁻¹ (the values in brackets are for the deuterated compound). The bending mode at 870 (621) cm⁻¹ shows an almost perfect 1/√2 wavenumber shift (0.71), while the stretching mode at 1211 (890) cm⁻¹ indicates some anharmonicity (0.73). The band at 431 cm⁻¹ corresponds to the external lattice mode highest in frequency (Al–Si in-plane stretching), which has almost zero intensity in the INS spectrum.

There are four atoms in the primitive unit cell of SrAlSiH and, hence, 12 normal modes of vibration. In addition to the acoustic modes, there are nine optic modes, which occur as three pairs of type A and double-degenerate type E. A and E manifest main displacements along *z* and in-plane *xy*, respectively. Internal [Al–H] modes (bending E and stretching A) are clearly separated from external lattice modes [Al and Si displaced along *z* in opposite directions (A) and in-plane Al–Si stretching (E); Sr vibrations against (A) and along puckered nets (E)]. The small dispersion of bands suggests modeling of the INS spectrum of SrAlSiH by optic modes at the Γ point only, which corresponds to a single unit cell (molecular) treatment. A spectrum was calculated with the program aCLIMAX¹⁷ using Γ -point phonon frequencies and displacements from first-principles calculations. By a slight scaling of the calculated frequencies toward experimental values, the Γ -point-approximated INS spectrum accounts perfectly for all features in the experimental spectrum (Figure 2a), apart from the LO–TO splitting of the degenerate [Al–H] bending mode, which is a consequence of the translational periodicity (see Figure 3 for calculated phonon dispersion curves). The internal modes give rise to overtones and combinations, and clearly resolved are the two quanta events around 1730 cm⁻¹ (bending-mode overtone), 2050 cm⁻¹ (combination mode), and 2300 cm⁻¹ (stretching-mode overtone; note again the apparent deviation from the harmonic approximation of this mode when comparing the calculated and experimental INS spectra).

For SrAl₂H₂, the number of internal modes is doubled (inset in Figure 2b) and they appear broadly dispersed in the INS spectrum. This dispersion is a consequence of H–H interactions between Al–H units from adjacent layers (which are not present in SrAlSiH). The band associated with the stretching mode is located between 1200 and 1500 cm⁻¹, and that associated with the bending mode is in a range between 500 and 750 cm⁻¹. Note that the bending-mode overtones overlap with the [Al–H] stretching band. The INS

- (11) (a) Kresse, G.; Furthmüller, J. *Phys. Rev. B* **1996**, *54*, 11169. (b) Kresse, G.; Furthmüller, J. *Comput. Mater. Sci.* **1996**, *6*, 15. Kresse, G.; Hafner, J. *Phys. Rev. B* **1993**, *47*, 558.
- (12) Vanderbilt, D. *Phys. Rev. B* **1990**, *41*, 7892.
- (13) Perdew, J. P.; Wang, Y. *Phys. Rev. B* **1992**, *45*, 13244.
- (14) Monkhorst, H. J.; Pack, J. D. *Phys. B* **1976**, *13*, 5188.
- (15) (a) Parlinski, K.; Li, Z.-Q.; Kawazoe, Y. *Phys. Rev. Lett.* **1997**, *78*, 4063. (b) Parlinski, K.; Li, Z.-Q.; Kawazoe, Y. *Phys. Rev. Lett.* **1998**, *81*, 3298.
- (16) (a) Dong, J.-J.; Sankey, O. F. *J. Phys.: Condens. Matter* **1999**, *11*, 6129. (b) Dong, J.-J.; Sankey, O. F. *J. Appl. Phys.* **2000**, *87*, 958. Nolas, G. S.; Kendziora, C. A.; Gryko, J.; Dong, J.; Myles, C.; Poddar, A.; Sankey, O. F. *J. Appl. Phys.* **2002**, *92*, 7225.
- (17) Ramirez-Cuesta, A. J. *Comput. Phys. Commun.* **2004**, *157*, 226.
- (18) The Cartesian *k*-points A, L, M, Γ , H, and K are (2 π /c)(0,0,¹/₂), (2 π /a)(¹/₂,¹/₂,¹/₂), (2 π /a)(¹/₂,¹/₂,0), (2 π /a)(¹/₂,0,0), (2 π /a)(0,¹/₂,0), and (2 π /a)(0,0,¹/₂), respectively.
- (19) The potential energy curves for molecules were computed using DFT-(B3LYP) with the 6-31G** basis set using the quantum chemistry code Dalton 2.0; DALTON, a molecular electronic structure program, release 2.0 (2005). <http://www.kjemi.uio.no/software/dalton/dalton.html>.

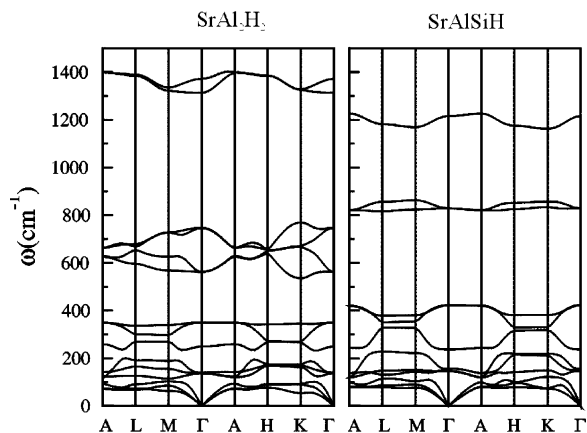


Figure 3. Calculated phonon dispersion curves for SrAl_2H_2 (left) and SrAlSiH (right) for the symmetry points of the Brillouin zone.¹⁸

Table 2. Calculated Phonon Frequencies (in cm^{-1}) for Optical Modes at the Γ Point (Equilibrium Lattice Parameters)

| mode type | SrAlSiH | SrAl_2H_2 |
|------------------------------------|------------------|---------------------------|
| E (Sr) | 146 | 136 |
| A (Sr) | 157 | 141 |
| A [Al–Si(Al) out-of-plane stretch] | 237 | 249 |
| E [Al–Si(Al) in-plane stretch] | 422 | 350 |
| E (Al–H bend) | 829 | 563 |
| E (Al–H bend) | | 747 |
| A (Al–H stretch) | 1215 | 1314 |
| A (Al–H stretch) | | 1372 |

spectrum of SrAl_2H_2 was calculated by employing computed frequencies and displacements across the Brillouin zone (i.e., considering phonon dispersion), and the agreement with the experimental spectrum is satisfactory (Figure 2b).

The calculated phonon dispersion curves and Γ -point wavenumbers are shown in Figure 3 and Table 2, respectively, and coincide very well with the measured vibrational spectra. The very small dispersion of the external modes of SrAlSiH is indeed remarkable and shows that [Al–H] entities in this compound can be considered as isolated, molecular-like. This is a truly unique phenomenon for a solid-state aluminum hydride. Interestingly, in SrAlSiH , [Al–H] bending modes appear at higher energy and stretching modes at lower energy, respectively, compared to SrAl_2H_2 . Finally, the external Al–Si in-plane stretching mode is at considerably higher energy [432/422 (exptl/calcd) cm^{-1}] than the corresponding Al–Al mode in SrAl_2H_2 (358/350 cm^{-1}), which indicates stronger bonding between atoms within the puckered hexagon nets for SrAlSiH .

We investigated further the anharmonicity of the Al–H stretching mode and calculated potential energy curves for SrAlSiH and SrAl_2H_2 and molecular AlH_3 (D_{3h}) and AlH_4^- (T_d).¹⁹ These curves are shown in Figure 4. For H displacements along the bond direction, the curves for molecules and solids all show significant anharmonicity. The potential energy curves for the displacement of a H atom along the hexagonal plane (x or y) for the solid hydrides are nearly harmonic, which is in agreement with the experiment. The potential energy curves were fitted to polynomials $U = ax^2 - bx^3 + cx^4$ (x is the displacement of a H atom in angstroms, and U is the energy in electronvolts). Table 3 shows the calculated energies for the ground state (E_0) and the first

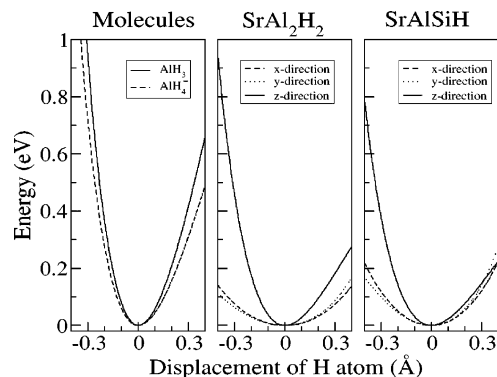


Figure 4. Potential energy curves for molecules (AlH_3 and AlH_4^-) and solids, SrAl_2H_2 and SrAlSiH . The H atom is more strongly bound in molecules than in solids. The potential curves show the anharmonic behavior for both the molecules and the solids when the H atom is displaced along the Al–H bonding axis (the z axis for solids).

Table 3. Numerically Calculated Energies for the Ground State (E_0), the First (E_1), and the Second (E_2) Excited States, and the Normal-Mode Frequencies ω_1 and ω_2 (in cm^{-1}) Using the Potential Energy Curve-Fit Polynomials from Figure 4^a

| | AlH_3 | AlH_4^- | SrAl_2H_2 | SrAlSiH |
|---------------------------------|----------------|------------------|---------------------------|------------------|
| E_0 (eV) | 0.1190 | 0.1029 | 0.0808 | 0.0726 |
| E_1 (eV) | 0.3517 | 0.3033 | 0.2346 | 0.2105 |
| E_2 (eV) | 0.5799 | 0.4996 | 0.3806 | 0.3434 |
| $\omega_1 = (E_1 - E_0)/\hbar$ | 1877 | 1616 | 1240 | 1112 |
| $\omega_2 = (E_2 - E_0)/\hbar$ | 3718 | 3199 | 2418 | 2184 |
| $\Delta = 2\omega_1 - \omega_2$ | 36 | 33 | 62 | 40 |

^a Only the Al–H stretching mode is considered. The frequency shift of the overtone (Δ) is related to the deviation from the harmonic approximation.

(E_1) and second (E_2) excited states, together with the corresponding transition frequencies ω_1 and ω_2 (overtone). Because of the anharmonicity, the overtone is shifted downward by Δ ($=2\omega_1 - \omega_2$). The computed Δ for SrAlSiH (40 cm^{-1}) is less than 50% that measured in the experiment (around 100 cm^{-1} ; cf. Figure 2a). Table 3 suggests that the experimentally observed anharmonic character of the Al–H stretch for SrAlSiH is also present in SrAl_2H_2 , and moreover in molecular aluminum hydrides, and is thus a general feature of the Al–H bond.

Some interesting conclusions can be drawn from this study. In both polyanionic aluminum hydrides, SrAl_2H_2 and SrAlSiH , H is bonded terminally to Al. However, the Al–H stretching modes, which are a direct measure of the bond strength, are at very low wavenumbers when compared to other solid-state^{7,20–26} or molecular aluminum hydrides with terminal Al–H bonds.^{27–29} This is shown in Figure 5. The

- (20) Iniguez, J.; Yildirim, T.; Udovic, T. J.; Sulic, M.; Jensen, C. M. *Phys. Rev. B* **2004**, *70*, 060101(R).
- (21) Wolverton, C.; Ozolins, V.; Asta, M. *Phys. Rev. B* **2004**, *69*, 144109.
- (22) Kolesnikov, A. I.; Adams, M.; Antonov, V. E.; Chirin, N. A.; Goremychkin, E. A.; Inikhova, G. G.; Markushkin, Y. E.; Prager, M.; Sashin, I. L. *J. Phys.: Condens. Matter* **1996**, *8*, 2529.
- (23) Ke, X.; Tanaka, I. *Phys. Rev. B* **2005**, *71*, 024117.
- (24) Ke, X.; Kuwabara, A.; Tanaka, I. *Phys. Rev. B* **2005**, *71*, 184107.
- (25) Peles, A.; Chou, M. Y. *Phys. Rev. B* **2006**, *73*, 184302.
- (26) Majzoub, E. H.; McCarty, K. F.; Ozolins, V. *Phys. Rev. B* **2005**, *71*, 024118.
- (27) Aldridge, S.; Downs, A. J. *Chem. Rev.* **2001**, *101*, 3305.
- (28) Andrews, L.; Wang, X. *Science* **2003**, *299*, 2049.
- (29) Pullumbi, P.; Bouteiller, Y.; Manceron, L. *J. Chem. Phys.* **1994**, *101*, 3610.

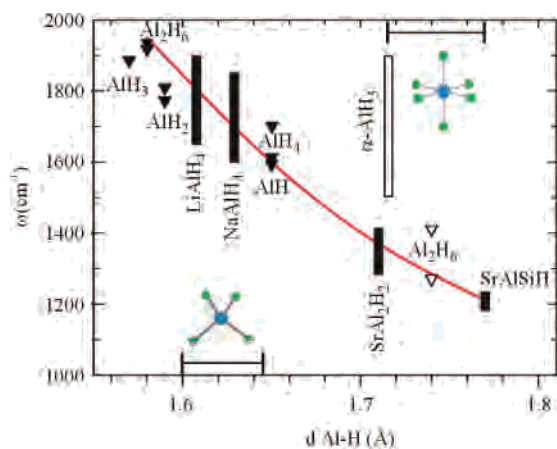


Figure 5. Compilation of experimentally obtained Al–H stretching frequencies over Al–H distances in various systems: triangles represent molecular compounds and extended bars (dispersed) solid-state systems. Open symbols indicate Al–H–Al bridging units and solid symbols terminal Al–H bonds. Two markers show the range of Al–H distances in tetrahedral $[\text{AlH}_4]$ and octahedral $[\text{AlH}_6]$ ensembles in solid-state hydrides. The red line is a guide to the eye.

molecular hydrides AlH , AlH_2 (C_{2v}), AlH_3 (D_{3h}), AlH_4^- (T_d), and Al_2H_6 (D_{2h}) and solid-state hydrides LiAlH_4 and NaAlH_4 ^{7,20,25,26} display [Al–H] stretches in a range between 1600 and 1950 cm^{-1} . Al_2H_6 has, in addition to terminal Al–H units, two Al–H–Al bridging units whose stretches appear at 1268 and 1408 cm^{-1} .²⁸ The terminal Al–H stretches of polyanionic SrAl_2H_2 compare to the wavenumbers of these bridging stretches.

Octahedral entities $[\text{AlH}_6]$ occur in alane, AlH_3 , alkali metal (A) alanates A_3AlH_6 ,³⁰ and alkaline-earth metal (Ae) alanates AeAlH_5 and Ae_2AlH_7 .³¹ The higher coordination number implies typically larger Al–H distances. Spectroscopic data for these systems are very sparse. $\alpha\text{-AlH}_3$ consists of corner-sharing $[\text{AlH}_6]$ octahedra, and its vibrational properties have been characterized by INS spectroscopy and first-principles calculations.^{21–23} The band associated with Al–H stretching is very dispersed and ranges from about 1500 to 1900 cm^{-1} . These are surprisingly high wavenumbers considering the fact that $\alpha\text{-AlH}_3$ exclusively consists of Al–H–Al bridges. On the contrary, for Na_3AlH_6 , which contains separated $[\text{AlH}_6]$ entities and terminal Al–H bonds, the stretching band appears dispersed over a region 1250–1550 cm^{-1} according to a calculated phonon density of states.²⁴ However, this result has not been ascertained experimentally.

(30) Graetz, J.; Lee, Y.; Reilly, J. J.; Park, S.; Vogt, T. *Phys. Rev. B* **2005**, *71*, 184115.

(31) (a) Zhang, Q.-A.; Nakamura, Y.; Oikawa, K.; Kamiyama, T.; Akiba, E. *Inorg. Chem.* **2002**, *41*, 6547. (b) Zhang, Q.-A.; Nakamura, Y.; Oikawa, K.; Kamiyama, T.; Akiba, E. *Inorg. Chem.* **2002**, *41*, 6941. (c) Weidenthaler, C.; Frankcombe, T. J.; Felderhoff, M. *Inorg. Chem.* **2006**, *45*, 3849.

The low [Al–H] stretching frequencies of SrAl_2H_2 and SrAlSiH imply that H is rather weakly bonded to Al. As a matter of fact, the frequency for SrAlSiH is the lowest hitherto observed for a terminal [Al–H] stretch. This low frequency is especially surprising when compared with SrAl_2H_2 because the presence of more electronegative Si has a polarizing effect on Al, which, in turn, should bind H more tightly. At the same time, SrAlSiH has the highest desorption temperature observed for an aluminum hydride. This apparent discrepancy can only be explained by compensating, strong, Sr–H interactions in SrAlSiH . The [Al–H] bending mode, where H displaces toward Sr atoms, reflects indirectly the strength of Sr–H interactions and will stiffen (i.e., shift to higher frequencies) for stronger Sr–H interactions. This is indeed the case for SrAlSiH . Furthermore, large portions of the phonon branches involving Sr atoms appear at considerably higher frequencies for SrAlSiH (cf. Figure 3). In both hydrides SrAl_2H_2 and SrAlSiH , Sr–H interactions should be considered as predominately ionic. However, while in metallic SrAl_2H_2 Sr is coordinated by six H atoms in an octahedral fashion, this coordination number is reduced to three in semiconducting SrAlSiH and Sr–H distances are considerably shorter.⁶

4. Conclusions

Novel polyanionic aluminum hydrides provide new coordination environments for H and demonstrate splendidly the complex interplay of different metal–H interactions in multicomponent metal hydride systems. They can play an important role as model systems for fundamental studies of Al–H bonding interactions. Alane (AlH_3) and alanates LiAlH_4 and NaAlH_4 that are currently investigated as hydrogen storage materials are thermodynamically only weakly stable or even metastable compounds.^{21,30} This makes reversibility of the decomposition reaction problematic. At the same time, these systems display strong Al–H bonding, as indicated in the high [Al–H] stretching frequencies. In more stable aluminum hydrides such as Na_3AlH_6 , SrAl_2H_2 , and SrAlSiH , Al–H bonding is weaker. It appears that the stability of solid-state aluminum hydrides correlates inversely with the strength of Al–H bonding. This can be explained by a more effective coordination of H in the latter systems due to the higher concentration of metal atoms present.

Acknowledgment. This work has been supported by the Swedish Research Council (VR). The Rutherford Appleton Laboratory is thanked for access to neutron beam facilities. We are grateful to Prof. Ulf Hälenius, Swedish Museum of Natural History, Stockholm, Sweden, for assistance with IR measurements.

IC700722B